Electron-vibron interactions in charged fullerenes. I. Berry phases

Assa Auerbach*
Physics Department, Technion, Haifa, Israel

Nicola Manini†
International School for Advanced Studies (SISSA), via Beirut 2-4, I-34013 Trieste, Italy

Erio Tosatti‡
International School for Advanced Studies (SISSA), via Beirut 2-4, I-34013 Trieste, Italy
and International Centre for Theoretical Physics (ICTP), P.O. Box 586, I-34014 Trieste, Italy
(Received 15 December 1993)

A simple model for electron-vibron interactions on charged fullerenes C_{60}^{n-}, $n=1,\ldots,5$, is solved both at weak and strong couplings. We consider a single H_g vibrational multiplet interacting with t_{1u} electrons. At strong coupling the semiclassical dynamical Jahn-Teller theory is valid. The Jahn-Teller distortions are unimodal for $n=1,2,4,5$ electrons, and bimodal for 3 electrons. The distortions are quantized as rigid-body pseudorotators which are subject to geometrical Berry phases. These impose ground-state degeneracies and dramatically change zero-point energies. Exact diagonalization shows that the semiclassical level degeneracies and ordering survive well into the weak-coupling regime. At weak coupling, we discover an enhancement factor of $\frac{5}{2}$ for the pair binding energies over their classical values. This has potentially important implications for superconductivity in fullerides, and demonstrates the shortcoming of Migdal-Eliashberg theory for molecular crystals.

I. INTRODUCTION

The spheroid-shaped molecule C_{60} (fullerene) and its various crystalline compounds have ignited enormous interest in the chemistry and physics community recently.[1] C_{60} is a truncated icosahedron. From a physicist's standpoint, the charged molecule is fundamentally interesting, because the high molecular symmetry gives rise to degeneracies in both electronic and vibrational systems. Thus, the molecule is very sensitive to perturbations. In particular, electron-phonon and electron-electron interactions are expected to produce highly correlated ground states and excitations.

Superconductivity has been discovered in alkali-metal-doped fullerenes A_3C_{60} (A=K,Cs,Rb), with relatively high transition temperatures ($T_c \approx 20$–30 K). There are experimental indications that the pairing mechanism originates in the electronic properties of a single molecule. The pair binding energy is a balance of electron-vibron interactions[2–4] and electron-electron interactions.[5] The relative contributions and signs of the two interactions are under some controversy.

The electron-vibron school has identified certain fivefold-degenerate H_g (d-wave-like) vibrational modes which couple strongly to the t_{1u} lowest unoccupied molecular orbital (LUMO).[2–4,6] Varma, Zaanen, and Raghavachari[2] as well as Schlüter *et al.* and, more recently, Antropov *et al.*[22] proposed that these modes undergo a Jahn-Teller (JT) distortion and calculated the induced pair binding energies at several fillings. They used the *classical approximation,* and restricted their calculation to unimodal distortions (defined later). The general conclusion of this approach is that, while the calculated λ is sizable, one still requires a large reduction of the Coulomb pseudopotential μ^* in order to explain the highest transition temperatures. On the other hand, Gunnarsson, Rainer, and Zwicknagl[23] independently estimate a large $\mu^* \approx 0.4$, i.e., there is no mechanism providing such a reduction.

However, estimates of the electron-vibron coupling constant g do not justify the classical JT approximation. C_{60} is estimated by frozen-phonon calculations to be in the weak-coupling regime $g \leq 1$ where quantum corrections are important.

In this paper (part I) we study the isolated C_{60}^{n-} charged molecule. In particular, we shall reconsider the same JT model, but diagonalize the quantum Hamiltonian for the full range of the coupling constant. We shall find that quantum corrections to the classical JT theory introduce novel qualitative features, and are quantitatively important for the pair binding energies.

The quantum fluctuations involve interference effects due to geometrical Berry phases. Berry phases appear in a wide range of physical phenomena.[7,8] Here we find the Berry phase in the context of a molecular Aharonov-Bohm (MAB) effect, originally discovered by Longuet-Higgins.[9] The MAB effect has important consequences on the vibron spectrum. For example, it produces half-odd integer quantum numbers in the spectrum of triangular molecules,[9,7] an effect recently confirmed spectroscopically in Na_3.[10] This kind of Berry phase is important also in scattering of hydrogen molecules.[11] Recently, it has been suggested that a geometrical Berry phase may be relevant in fullerene ions.[12–14] Here we show that Berry phases produce *selection rules* for the pseudorotational quantum numbers and *kinematical* restrictions

which affect the pairing interaction between electrons. Although the semiclassical and Berry-phase description is appropriate in strong coupling, the level ordering and degeneracies are found to survive for arbitrary coupling, particularly in the weak-coupling regime, which is closer to actual C_{60}. For this reason we devote a large portion of this paper to the semiclassical theory, which helps to build physical intuition for further extensions of the model.

This paper is organized as follows: In Sec. II the basic model is introduced. Section III calculates the JT distortions in the classical limit. Section IV derives the semiclassical quantization about the JT manifold. The geometrical Berry phases are calculated, and their effect on the semiclassical spectrum is obtained up to order g^{-2}. Section V describes the exact diagonalization results, and compares them to the semiclassical theory, and to weak-coupling perturbation theory. The pair binding energies are determined in Sec. VI. In Sec. VII we summarize the paper and discuss our main result: that the effective pair binding energies are larger by a factor of 3 than the pair interaction energy in Migdal-Eliashberg theory. In the following paper[15] we shall extend the model to all A_g and H_g modes with realistic physical parameters. This will allow us to explore the experimental consequences of the electron-vibron interactions.

II. THE ELECTRON-VIBRON MODEL

The single-electron LUMO states of C_{60} are in a triplet of t_{1u} representation. We consider the H_g (five-dimensional) vibrational multiplet which couples to these electrons. t_{1u} and H_g are the icosahedral-group counterparts of the spherical harmonics $\{Y_{1m}\}_{m=-1}^{1}$ and $\{Y_{2m}\}_{M=-2}^{2}$, respectively. By replacing the truncated icosahedron symmetry group by the spherical group, we ignore lattice corrugation effects. These are expected to be small since they do not lift the degeneracies of the $L=1,2$ representations.

The Hamiltonian is thus defined as

$$H=H^0+H^{e\text{-}v}\ , \tag{1}$$

where

$$H^0=\hbar\omega\sum_M (b_M^\dagger b_M+\tfrac{1}{2})+(\epsilon-\mu)\sum_{ms} c_{ms}^\dagger c_{ms}\ . \tag{2}$$

$b_M^\dagger$ creates a vibron with azimuthal quantum number M, and $c_{ms}^\dagger$ creates an electron of spin s in an orbital Y_{1m}. We fix the number of electrons to be n, and set the chemical potential $\mu\to\epsilon$, which discards the second term.

The H_g vibration field is

$$u(\hat\Omega)=\frac{1}{\sqrt{2}}[Y_{2m}^*(\hat\Omega)b_M^\dagger+Y_{2M}(\hat\Omega)b_M]\ , \tag{3}$$

where $\hat\Omega$ is a unit vector on the sphere. The t_{1u} electron field is

$$\psi_s(\hat\Omega)=\sum_{m=-1}^{1} Y_{1m}(\hat\Omega)c_{ms}\ . \tag{4}$$

The electron-vibron interaction is local and rotationally invariant. Its form is completely determined (up to an overall coupling constant g) by symmetry:

$$H^{e\text{-}v}\propto g\int d\hat\Omega u(\hat\Omega)\sum_s \psi_s^\dagger(\hat\Omega)\psi_s(\hat\Omega)\ . \tag{5}$$

Using the relation

$$\int d\hat\Omega Y_{LM}(\hat\Omega)Y_{lm_1}(\hat\Omega)Y_{lm_2}(\hat\Omega)\propto(-1)^M\langle L,-M|lm_1;lm_2\rangle\ , \tag{6}$$

where $\langle\cdots\rangle$ is a Clebsch-Gordan coefficient,[16] yields the second quantized Hamiltonian

$$H^{e\text{-}v}=\frac{\sqrt{3}}{2}g\hbar\omega\sum_{s,M,m}(-1)^m[b_M^\dagger+(-1)^M b_{-M}]\times\langle 2,M|1,-m;1,M+m\rangle\times c_{ms}^\dagger c_{M+ms}\ . \tag{7}$$

The coupling constant g is fixed by the convention of O'Brien, who studied this kind of dynamical JT problem.[17] Representation (7) is convenient for setting up an exact diagonalization program in the truncated Fock space.

The real representation

The semiclassical expansion is simpler to derive in the real-coordinates representation. The vibron coordinates are

$$q_\mu=\frac{6}{\sqrt{10}}\sum_{m=-2}^{2} M_{\mu m}[b_m^\dagger+(-1)^m b_{-m}]\ , \tag{8}$$

where

$$M_{\mu,m\neq 0}=[2\,\mathrm{sgn}(\mu)]^{-1/2}[\delta_{\mu,m}+\mathrm{sgn}(\mu)\delta_{\mu,-m}]\ ,\qquad M_{\mu,0}=\delta_{\mu,0}\ . \tag{9}$$

$\{q_\mu\}$ are coefficients of the real spherical functions

$$f_\mu(\hat\Omega)=\frac{6}{\sqrt{5}}\sum_m M_{\mu,m}Y_{2m}(\hat\Omega)=\begin{cases}\frac{6}{\sqrt{10}}\mathrm{Re}[Y_{2|\mu|}(\hat\Omega)], & \mu=1,2\ ,\\ \frac{6}{\sqrt{5}}Y_{20}(\hat\Omega), & \mu=0\ ,\\ \frac{6}{\sqrt{10}}\mathrm{Im}[Y_{2|\mu|}(\hat\Omega)], & \mu=-1,-2\ .\end{cases} \tag{10}$$

We also choose a real representation for the electrons,

$$c_{xs}^\dagger=\frac{1}{\sqrt{2}}(c_{1s}^\dagger+c_{-1s}^\dagger)\ ,\qquad c_{ys}^\dagger=\frac{1}{i\sqrt{2}}(c_{1s}^\dagger-c_{-1s}^\dagger)\ ,\qquad c_{zs}^\dagger=c_{0s}^\dagger\ . \tag{11}$$

Thus the Hamiltonian in the real representation is given by

$$H=H^0+H^{e\text{-}v}\ ,$$

$$H^0=\frac{\hbar\omega}{2}\sum_\mu(-\partial_\mu^2+q_\mu^2)\ , \tag{12}$$

$$H^{e\text{-}v}=g\frac{\hbar\omega}{2}\sum_s(c_{xs}^\dagger,c_{ys}^\dagger,c_{zs}^\dagger)\times\begin{bmatrix}q_0+\sqrt{3}q_2 & -\sqrt{3}q_{-2} & \sqrt{3}q_1\\ -\sqrt{3}q_{-2} & q_0-\sqrt{3}q_2 & -\sqrt{3}q_{-1}\\ -\sqrt{3}q_1 & \sqrt{3}q_{-1} & -2q_0\end{bmatrix}\times\begin{bmatrix}c_{xs}\\ c_{ys}\\ c_{zs}\end{bmatrix}.$$

This form of the JT Hamiltonian is well known.[17,2] Since the Hamiltonian is rotationally invariant, its eigenvalues are invariant under simultaneous O(3) rotations of the electronic and vibronic representations.

III. JAHN-TELLER DISTORTIONS (CLASSICAL)

In the classical limit, one can ignore the vibron derivative terms in (12), and treat $\vec{q}=\{q_\mu\}$ as frozen coordinates in $H^{e\text{-}v}$. The coupling matrix in $H^{e\text{-}v}$ is diagonalized by[18]

$$T^{-1}(\varpi)\begin{bmatrix}z-\sqrt{3}r & 0 & 0\\ 0 & z+\sqrt{3}r & 0\\ 0 & 0 & -2z\end{bmatrix}T(\varpi)\ , \tag{13}$$

where

$$T=\begin{bmatrix}\cos\psi & \sin\psi & 0\\ -\sin\psi & \cos\psi & 0\\ 0 & 0 & 1\end{bmatrix}\begin{bmatrix}\cos\theta & 0 & \sin\theta\\ 0 & 1 & 0\\ \sin\theta & 0 & \cos\theta\end{bmatrix}\times\begin{bmatrix}\cos\phi & \sin\phi & 0\\ -\sin\phi & \cos\phi & 0\\ 0 & 0 & 1\end{bmatrix}. \tag{14}$$

$\varpi=(\phi,\theta,\psi)$ are the three Euler angles of the O(3) rotation matrix T. In the diagonal basis of (13), the electron energies depend only on two vibron coordinates:

$$\vec{q}(0)=\begin{bmatrix}r\\0\\z\\0\\0\end{bmatrix}. \tag{15}$$

By rotating the vibron coordinates $\vec{q}$ to the diagonal basis using the $L=2$ rotation matrix $D^{(2)}$,[16] one obtains

$$\vec{q}_\mu(r,z,\varpi)=\sum_{m,m',\mu'=-2}^{3}M_{\mu,m}D^{(2)}_{m,m'}(\varpi)M^{-1}_{m'\mu'}\vec{q}_{\mu'}(0)\ , \tag{16}$$

where $M_{\mu,m}$ was defined in (9).

By (16), and the unitarity of D and M, $|\vec{q}|^2$ is invariant under rotations of ϖ. Thus, the adiabatic potential energy V depends only on r, z, and the occupation numbers of the electronic eigenstates n_i, where $\sum_i n_i=n$.

$$V(z,r,[n_i])=\frac{\hbar\omega}{2}(z^2+r^2)+\frac{\hbar\omega g}{2}[n_1(z-\sqrt{3}r)+n_2(z+\sqrt{3}r)-n_3 2z]\ . \tag{17}$$

V is minimized at the JT distortions $(\bar{z}_n,\bar{r}_n,\bar{n}_i)$, at which the classical energy is given by

$$E_n^{\rm cl}=\min V(\bar{z}_n,\bar{r}_n,\bar{n}_i)\ . \tag{18}$$

The JT distortions at different fillings are given in Table I. We define $\tilde{\phi},\tilde{\theta}$ as the longitude and latitude with respect to the diagonal frame ("principal axes") labeled (1,2,3) (3 is at the north pole). $\bar{z},\bar{r}$ parametrize the Jahn-Teller distortion in the real representation (10), as

$$\langle u^{\rm JT}(\tilde{\theta},\tilde{\phi})\rangle=\frac{\bar{z}}{2}(3\cos^2\tilde{\theta}-1)+\frac{\bar{r}\sqrt{3}}{2}\sin^2\tilde{\theta}\cos(2\tilde{\phi})\ . \tag{19}$$

In Table I we present the values of the ground-state JT distortions at all electron fillings. We see that electron fillings $n=1,2,4,5$ have *unimodal* distortions which are symmetric about the 3 axis, while $n=3$ has a *bimodal*

TABLE I. Semiclassical ground-state distortions and energies for a single H_g coupled mode of frequency ω. n is the electron number, S is the total spin, $\bar{z}_n$, $\bar{r}_n$ are the JT distortions, $\bar{n}_i$ is the occupation of orbital i, E_n is the ground-state energy, and U_n is the pair energy [Eq. (50)]. Energies are calculated for strong coupling to order g^{-2}.

n	S	$(\bar{z}_n,\bar{r}_n)$	$(\bar{n}_1,\bar{n}_2,\bar{n}_3)$	$E_n/(\hbar\omega)$	$U_n/(\hbar\omega)$
0	0	(0,0)	(0,0,0)	$\frac{5}{2}$	
1	$\frac{1}{2}$	$(g,0)$	(0,0,1)	$-\frac{1}{2}g^2+\frac{3}{2}+\frac{1}{3g^2}$	$-g^2+1-\frac{2}{3g^2}$
2	0	$(2g,0)$	(0,0,2)	$-2g^2+\frac{3}{2}$	
3	$\frac{1}{2}$	$\left(\frac{3}{2}g,\frac{\sqrt{3}}{2}g\right)$	(1,0,2)	$-\frac{3}{2}g^2+1+\frac{1}{3g^2}$	$-g^2+1-\frac{2}{3g^2}$
4	0	$(-2g,0)$	(2,2,0)	$-2g^2+\frac{3}{2}$	
5	$\frac{1}{2}$	$(-g,0)$	(2,2,1)	$-\frac{1}{2}g^2+\frac{3}{2}+\frac{1}{3g^2}$	$-g^2+1-\frac{2}{3g^2}$
6	0	(0,0)	(2,2,2)	$\frac{5}{2}$	

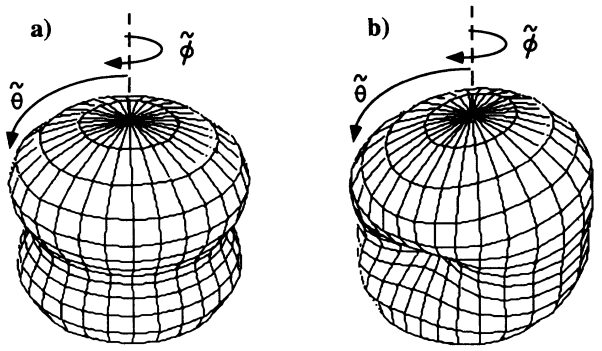

FIG. 1. Polar representation of the Jahn-Teller distortions $u^{\mathrm{JT}}(\tilde{\theta},\tilde{\phi})$, Eq. (19). The distortion is measured relative to a sphere. (a) The unimodal distortion for the ground states of $n=1,2,4,5$ electrons; (b) the bimodal distortion for $n=3$ electrons.

distortion, about the 3 and 1 axes. The two types of distortions are portrayed in Fig. 1, where we depict the distortions of (19) for the unimodal and bimodal cases.

IV. SEMICLASSICAL QUANTIZATION

At finite coupling constant g, quantum fluctuations about the frozen JT distortion must be included. In order to carry out the semiclassical quantization, we define a natural set of five-dimensional coordinates r,z,ϖ. ϖ parametrize the motion in the JT manifold (the valley in the "mexican hat" potential V) and r,z are transverse to the JT manifold, since V depends on them explicitly. The transformation $\vec{q}(r,z,\varpi)$ was given in (16), and was derived explicitly in Ref. 18 to be

$$\begin{aligned}
q_2 &= z\tfrac{1}{2}\sqrt{3}\sin^2\theta\cos^2\phi + r\tfrac{1}{2}(1+\cos^2\theta)\cos2\phi\cos2\psi \\
&\quad - r\cos\theta\sin2\phi\sin2\psi \ , \\
q_1 &= z\tfrac{1}{2}\sqrt{3}\sin2\theta\cos\phi - r\tfrac{1}{2}\sin2\theta\cos\phi\cos2\psi \\
&\quad + r\sin\theta\sin\phi\sin2\psi \ , \\
q_0 &= z\tfrac{1}{2}(3\cos^2\theta-1) + \bar{r}\tfrac{1}{2}\sqrt{3}\sin^2\theta\cos2\psi \ , \\
q_{-1} &= z\tfrac{1}{2}\sqrt{3}\sin2\theta\sin\phi - r\tfrac{1}{2}\sin2\theta\sin\phi\cos2\psi \\
&\quad - r\sin\theta\cos\phi\sin2\psi \ , \\
q_{-2} &= z\tfrac{1}{2}\sqrt{3}\sin^2\theta\sin2\phi + r\tfrac{1}{2}(1+\cos^2\theta)\sin2\phi\cos2\psi \\
&\quad - r\cos\theta\cos2\phi\sin2\psi \ .
\end{aligned} \tag{20}$$

The velocity in R^5 is given by

$$\dot{\vec{q}}(r(t),z(t),\varpi(t)) = \partial_r\vec{q}\dot{r} + \partial_z\vec{q}\dot{z} + \partial_\varpi\vec{q}\cdot\dot{\varpi} \ . \tag{21}$$

Using (20) and (21), we calculate the classical kinetic energy in terms of the JT coordinates. After some cumbersome, but straightforward, algebra the kinetic energy is obtained in the compact and instructive form:

$$\begin{aligned}
\tfrac{1}{2}|\dot{\vec{q}}|^2 &= \frac{1}{2}\left[\dot{z}^2+\dot{r}^2+\sum_{i=1}^{3} I_i\omega_i^2\right] , \\
\omega_1 &= -\sin\psi\dot{\theta}+\cos\psi\sin\theta\dot{\phi} \ , \\
\omega_2 &= \cos\psi\dot{\theta}+\sin\psi\sin\theta\dot{\phi} \ , \\
\omega_3 &= \dot{\psi}+\cos\theta\dot{\phi} \ , \\
(I_1,I_2,I_3) &= [(\sqrt{3}z+r)^2,(\sqrt{3}z-r)^2,4r^2] \ .
\end{aligned} \tag{22}$$

For finite JT distortions, we can identify the Euler-angle terms as the kinetic energy of a rigid-body rotator,[19] and the quantities $I_i(\bar{z},\bar{r})$ as moments of inertia in the principal-axes frame (1,2,3). Thus, the Euler-angle dynamics follows that of a *rigid-body rotator*.[16] The unimodal and bimodal cases will be discussed separately.

A. Unimodal distortions

For the unimodal cases (which we found for the ground states of $n=1,2,4,5$, $\bar{r}=0$ on the JT manifold), the "moments of inertia" in (22) are given by the tensor

$$\hat{I} = 3\bar{z}^2\begin{bmatrix}1&0&0\\0&1&0\\0&0&0\end{bmatrix} . \tag{23}$$

This corresponds to the rotational energy of a point particle on a sphere, which is described by the angles θ,ϕ, and moment of inertia $3\bar{z}^2$. Since axis 3 has no "mass," its angular velocity is dominated by $\dot{\psi}$. This implies that we must keep the term $r^2\dot{\psi}^2$ but can discard the smaller mixed terms $\dot{\psi}\dot{\phi}$. This yields

$$\tfrac{1}{2}|\dot{\vec{q}}|^2 \approx \tfrac{1}{2}[\dot{z}^2+\dot{r}^2+r^2(2\dot{\psi})^2+3\bar{z}^2(\dot{\theta}^2+\sin^2\theta\dot{\phi}^2)] \ . \tag{24}$$

The angular velocity $\dot{\psi}$ couples to r^2 as in the kinetic energy of a three-dimensional vector $\mathbf{r}$ parametrized by the cylindrical coordinates

$$\mathbf{r} = [r\cos(2\psi), r\sin(2\psi), z-\bar{z}] \ . \tag{25}$$

For $|\mathbf{r}| \ll \bar{z}$, the potential is simply

$$V(\mathbf{r}) \approx \tfrac{1}{2}|\mathbf{r}|^2 \ . \tag{26}$$

Thus, the semiclassical Hamiltonian of the unimodal distortion is

$$\begin{aligned}
H^{\mathrm{uni}} &\approx H^{\mathrm{rot}} + H^{\mathrm{HO}} \ , \\
H^{\mathrm{rot}} &= \frac{\hbar\omega}{6\bar{z}^2}\vec{L}^2 \ , \\
H^{\mathrm{HO}} &= \hbar\omega\sum_{\gamma=1}^{3}(a_\gamma^\dagger a_\gamma + \tfrac{1}{2}) \ ,
\end{aligned} \tag{27}$$

where $\vec{L}$ is an angular momentum operator, and H^{HO} are the three harmonic-oscillator modes of $\mathbf{r}$. The energies are given by

$$E^{\mathrm{uni}} = \hbar\omega\left[\frac{1}{6\bar{z}_n^2}L(L+1)+\sum_{\gamma=1}^{3}(n_\gamma+\tfrac{1}{2})\right] . \tag{28}$$

The rotational part of the eigenfunctions is

$$\Psi^{\rm rot}_{Lm}(\vec{q})=Y_{Lm}(\hat{\Omega})|[n_{is}]\rangle_{\hat{\Omega}} , \tag{29}$$

where $\hat{\Omega}=(\theta,\phi)$ is a unit vector, and $|[n_{is}]\rangle_{\hat{\Omega}}$ is the electronic adiabatic ground state. It is a Fock state in the *principal-axes* basis. In terms of the stationary Fock basis $|[n_{\alpha s'}]\rangle$ where $\alpha=x,y,z$, the adiabatic ground state is

$$|[n_{is}]\rangle_{\hat{\Omega}}=\sum_{[n_{\alpha s}]}\langle[n_{\alpha s}]|[n_{is}]\rangle_{\hat{\Omega}}|[n_{\alpha s}]\rangle . \tag{30}$$

Each overlap is a Slater determinant which is a sum of n products of spherical harmonics

$$\langle[n_{\alpha s}]|[n_{is}]\rangle_{\hat{\Omega}}=\sum_{[\nu]}C_{[\nu]}Y_{1\nu_1}(\hat{\Omega})Y_{1\nu_2}(\hat{\Omega})\cdots Y_{1\nu_n}(\hat{\Omega}) , \tag{31}$$

where $C_{[\nu]}$ are constants.

Now we discuss how boundary conditions determine the allowed values of L. A reflection on the JT manifold is given by

$$\hat{\Omega}\rightarrow-\hat{\Omega} . \tag{32}$$

Spherical harmonics are known to transform under reflection as

$$Y_{Lm}\rightarrow(-1)^L Y_{Lm} . \tag{33}$$

Thus, by (30) and (31), the electronic part of the wave function transforms as

$$|[n_{is}]\rangle_{\hat{\Omega}}\rightarrow(-1)^n|[n_{is}]\rangle_{-\hat{\Omega}} . \tag{34}$$

The reflection (32) can be performed by moving on a *continuous path* on the sphere from any point to its opposite (see Fig. 2). It is easy to verify, using (16) or (20), that this path is a *closed orbit* of $\vec{q}\in R^5$:

$$\vec{q}(\hat{\Omega})\rightarrow\vec{q}(-\hat{\Omega})=\vec{q}(\hat{\Omega}) . \tag{35}$$

Thus we find that the electronic wave function yields a *Berry-phase factor* of $(-1)^n$ for rotations between opposite points on the sphere which correspond to closed orbits of $\vec{q}$. In order to satisfy (29) using the invariance of the left-hand side under reflection, the pseudorotational

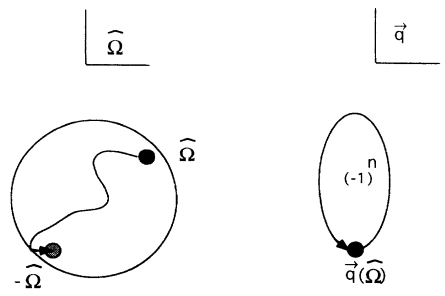

FIG. 2. Berry-phase calculation for unimodal distortions. A path between reflected points on the unit sphere corresponds to a closed orbit in the five-dimensional $\vec{q}$ space. According to Eq. (34), such a path acquires a Berry phase of $(-1)^n$ from the n-electron wave function.

Y_{Lm} wave function must cancel the electronic Berry phase. This amounts to a *selection rule* on L:

$$(-1)^{L+n}=1 . \tag{36}$$

Thus, the ground state for $n=1$ and 5 electrons has pseudo-angular-momentum $L=1$ and finite zero-point energy due to the nontrivial Berry phases.

B. Bimodal distortion

The analysis of the bimodal distortions $n=3$ proceeds along similar lines. The distortion obeys

$$\bar{z}=\sqrt{3}\bar{r} . \tag{37}$$

From Eq. (22) we see that the kinetic energy is given by

$$\tfrac{1}{2}|\dot{\vec{q}}|^2=\frac{1}{2}\left[\dot{z}^2+\dot{r}^2+\sum_{i=1}^{3}I_i\omega_i^2\right] , \tag{38}$$

where the inertia tensor is

$$\hat{I}=2\bar{z}^2\begin{bmatrix}4&0&0\\0&1&0\\0&0&1\end{bmatrix} . \tag{39}$$

The quantization of the pseudorotational part is the quantum-symmetric top Hamiltonian. Fortunately, it is a well-known textbook problem (see, e.g., Refs. 20 and 16). The eigenfunctions of a rigid-body rotator are the rotational matrices

$$D^{(L)}_{mk}(\varpi) , \tag{40}$$

where L,m,k are quantum numbers of the commuting operators $\vec{L}^2$, L^z, L^1, respectively. L^z and L^1 are defined with respect to the fixed z axis and the corotating 1 axis respectively. The quantum numbers are in the ranges

$$\begin{aligned}&L=0,1,\ldots,\infty ,\\&m,k=-L,-L+1,\ldots,L .\end{aligned} \tag{41}$$

The remaining coordinates are two massive harmonic-oscillator modes

$$\mathbf{r}=(r-\bar{r},z-\bar{z}) . \tag{42}$$

The semiclassical Hamiltonian is thus

$$\begin{aligned}&H^{\rm bi}\approx H^{\rm rot}+H^{\rm HO} ,\\&H^{\rm rot}=\frac{\hbar\omega}{4\bar{z}^2}\vec{L}^2-\frac{3\hbar\omega}{16\bar{z}^2}(L^1)^2 ,\\&H^{\rm HO}=\hbar\omega\sum_{\gamma=1}^{2}(a^\dagger_\gamma a_\gamma+\tfrac{1}{2}) ,\end{aligned} \tag{43}$$

and its eigenvalues are

$$E^{\rm bi}=\hbar\omega\left[\frac{1}{4\bar{z}^2}L(L+1)-\frac{3}{16\bar{z}^2}k^2+\sum_{\gamma=1}^{2}(n_\gamma+\tfrac{1}{2})\right] . \tag{44}$$

The rotational eigenfunctions are explicitly dependent on ϖ as

$$\Psi^{\rm rot}_{Lmk}[\vec{q}\,]=D^{(L)}_{mk}(\varpi)\prod_{is}|n_{is}\rangle_{\varpi}\ . \tag{45}$$

C. Berry phases of a bimodal distortion

Unlike the unimodal case, in the bimodal case no single reflection fully classifies the symmetry of the wave function. However, one can obtain definite sign factors by transporting the electronic ground state in certain orbits. We define the rotations of π about the principal axis L^i as C_i, which are schematically depicted in Fig. 3. The Berry phases associated with these rotations can be read directly from the rotation matrix T in Eq. (14). For example, for $\psi\rightarrow\psi+\pi$ (C_3), the states $|1\rangle$ and $|2\rangle$ get multiplied by (-1).

Since $D^{(L)}_{m,k}$ transform as Y_{Lk} under C_i, it is easy to determine the sign factors of the pseudorotational wave function. The results are given below:

$$\begin{aligned}
&C_1\colon\ |1,0,2\rangle_{\varpi}\rightarrow|1,0,2\rangle_{\varpi'}\ ,\\
&C_2\colon\ |1,0,2\rangle_{\varpi}\rightarrow-|1,0,2\rangle_{\varpi'}\ ,\\
&C_3\colon\ |1,0,2\rangle_{\varpi}\rightarrow-|1,0,2\rangle_{\varpi'}\ ,
\end{aligned} \tag{46}$$

$$\begin{aligned}
&C_1\colon\ D^{(L)}_{m,k}\rightarrow(-1)^k D^{(L)}_{m,k}\ ,\\
&C_2\colon\ D^{(L)}_{m,k}\rightarrow(-1)^{L+k} D^{(L)}_{m,-k}\ ,\\
&C_3\colon\ D^{(L)}_{m,k}\rightarrow(-1)^{L} D^{(L)}_{m,-k}\ .
\end{aligned}$$

$\vec{q}$ are coefficients in an $L=2$ representation, and therefore are invariant under C_1,C_2,C_3. C_i describe continuous closed orbits in R^5. In order to satisfy (46) and using the degeneracy of $E^{\rm bi}$ for $k\rightarrow-k$, we find that

$$L=\text{odd},\quad k=\text{even}\ . \tag{47}$$

In particular, the ground state of (45) is given by $L=1$ and $k=0$.

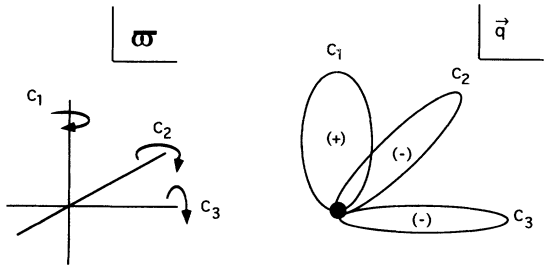

FIG. 3. Berry-phase calculation for the bimodal distortion ($n=3$). ϖ are the three Euler angles which rotate the principal axes of the bimodal distortion. C_i denote rotations by π around corresponding axes. On the right we depict the electronic Berry phases associated with the three closed orbits in $\vec{q}$ space, given by Eq. (46).

TABLE II. High-spin ground-state properties, in the same notation as Table I.

n	S	$(\bar{z}_n,\bar{r}_n)$	$(\bar{n}_1,\bar{n}_2,\bar{n}_3)$	$E_n/(\hbar\omega)$
2	1	$(-g,0)$	(1,1,0)	$-\frac{1}{2}g^2+\frac{3}{2}$
3	$\frac{3}{2}$	(0,0)	(1,1,1)	$\frac{5}{2}$
4	1	$(g,0)$ (uni)	(1,1,2)	$-\frac{1}{2}g^2+\frac{3}{2}$

D. High-spin-polarized ground states

It is possible to repeat the semiclassical analysis assuming that the spins are maximally polarized. These high-spin states are important, as they tend to prevail for strongly repulsive intralevel Hubbard-U (Hund's rule) situations. In this case, we determine the JT distortions considering the Pauli exclusion between likewise spins. In Table II the JT distortions of the spin-polarized ground states are listed. Our results for the $n=2,4$ ($S=1$) and $n=3$ ($S=\frac{3}{2}$) cases are presented. The latter is trivial, since in that case $n_1=n_2=n_3=1$, and therefore there is no JT effect at all. For $n=2$ ($S=1$), there is unimodal distortion of $\bar{z}=-g$ which is smaller than the unpolarized ground state, and is equal to the distortion of the $n=5$ case. Inspection of the orbital energies $\epsilon_1=\epsilon_2=-g$, $\epsilon_3=2g$ provides a clear explanation for the identical distortions of the $n=2$ ($S=1$) and $n=5$ ($S=\frac{1}{2}$) cases, since in both cases ϵ_3 is occupied by a spin-up hole.

Electronically, however, the two states are very different. First, we do not have a Berry phase for even number of electrons, as the individual contributions from each of the two electrons cancel out. Second, there is a nonzero *electronic* orbital angular momentum. For example, the symmetry of the two-electron state prior to JT distortion is ^3P (i.e., $^3t_{1u}$), and so it remains following dynamical JT distortion.[21] At finite coupling the two electrons in their ground states are still coupled in a ^3P electronic state, with $L_{\rm orb}=1$, where $L_{\rm orb}$ is the electronic orbital angular momentum, not to be confused with the pseudorotational quantum number L. Due to the absence of a Berry phase, L must in fact be even, in contrast with the single-electron case, and in agreement with Eq. (36). Thus, although both cases have threefold degeneracies, they arise from different physical motion: purely electronic (for the $n=2$, $S=1$ case) versus mixed electron-vibron motion (in the $n=5$, $S=\frac{1}{2}$ case).

V. EXACT DIAGONALIZATION

The above semiclassical scheme gives a clear and intuitive picture of the behavior of the system in the strong-coupling limit. This limit is appropriate for describing, e.g., Na_3.[10] However, in C_{60} the actual range of the coupling parameter—$g\approx0.3$ for a typical mode[22,15]—suggests that the electron-vibron coupling is actually in the weak-to-intermediate regime.

Here we diagonalize the electron-vibron Hamiltonian (7) for a single H_g mode in a truncated Fock space. This approach yields accurate results unless the coupling strength is too large, and the higher excited vibrons ad-

mix strongly into the low-lying states. We compare the results to the asymptotic large-g expressions of the semiclassical approximation. The ground-state energy for $n=1$ has been previously computed in this fashion by O'Brien.[18] Here we present detailed results for all electron occupations, and also for the excitation spectra.

Our basis is the finite-dimensional Fock space of electrons and vibrons,

$$\left\{ |n_M, n_{ms}\rangle :\ N_v \le N^{\max},\ \sum_{ms} n_{ms} = n \right\}, \tag{48}$$

where $N_v = \sum_M n_M$ is the total vibron occupation. By gradually increasing $N^{\max}$, we have found empirically that accurate results can be obtained for $g \le N^{\max}/2$, for levels with unperturbed energy below $\hbar\omega N^{\max}/2$. In particular, we have chosen $N^{\max}=5$ (for $n=2,3$), which yields an accuracy of better than $0.05\hbar\omega$ for $g \le 0.6$ and levels with $N_v \le 1$. The effect of truncation is a general upward shift of the levels, which gradually increases for higher excited levels. Level splittings and excitation energies are therefore less sensitive to the cutoff error.

In Figs. 4, 5, and 6 below, the energies of the ground state and a few of the excited states are plotted for one, two, and three electrons, respectively. The four- and five-electron spectra are related to the two- and one-electron spectra by particle-hole symmetry. Energies are plotted as functions of g^2. We compare the results to the semiclassical expressions (28) and (44) for large coupling, and to second-order perturbation theory at weak coupling. We discuss the different cases in detail, below.

A. $n=1,5$ electrons

The ground state for one electron or hole in the t_{1u} shell is a threefold-degenerate state (all degeneracies given do not include spin) of the same symmetry: this fact is in complete analogy with what happens in the $e\otimes E$ coupled system, where the final dynamical JT-coupled ground state has again E symmetry.[21] Additional splitting of this ground state could occur via spin-orbit coupling, not included in the present treatment. Recent spectroscopic data[24] of C_{60}^- embedded in solid Ar confirm indirectly the presence of the pseudorotational $L=1$ ground-state degeneracy, with possible spin-orbit splittings of about 30 and 75 cm^{-1} for the t_{1u} ground state and for the t_{1g} excited electronic state ≈ 1 eV above. The decrease of the ground-state energy is initially fast, and becomes gradually slower for increasing g. We shall return to this point in detail in the following paper.[15]

As shown in Fig. 4, for large g, the $n=1$ ground-state energy correctly approaches the strong-coupling limit,

$$E \sim -\frac{1}{2}g^2 + \frac{3}{2} + \frac{1}{3g^2}, \tag{49}$$

except for a small shift due, as mentioned above, to a finite-cutoff error. Above the ground state, there are families of excitations, corresponding to increasing values of N_v. The lowest, for $N_v=1$, comprises $3\times 5=15$ states, since for $n=1$, $N_v=1$ there are just three electron states

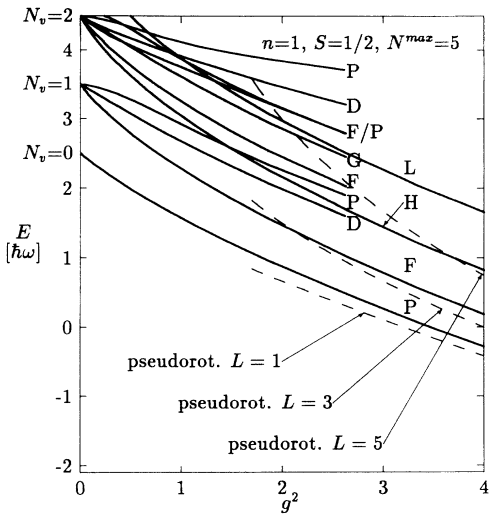

FIG. 4. Exact spectrum for one electron as a function of the square of the electron-vibron coupling constant g^2. The vibron occupations are truncated at $N^{\max}=5$. The semiclassical energies [Eq. (28)] are drawn by dashed lines for the lowest three pseudorotational multiplets ($n_\gamma=0, L=1,3,5$). The unit of energy is the vibron quantum $\hbar\omega$.

and five vibron states available. These states correspond to a direct product of a P (electronic) and a D (vibrational) manifold. As elementary angular momentum theory requires, they split into $L=3$, 2, and 1 levels, which are found, in order of increasing energy. The splitting initially is proportional to g^2, for small g, with significant deviations from linearity at $g^2 \approx 0.2$. As coupling increases, we note the slower downward trend of the *even-L* states, than both the ground state and the associated "soft" odd-L excitations. This clearly reflects the Berry-phase selection rule (36) that *no even L should appear among the low-lying excited states* in strong coupling. The lowest excitation from the ground state is $L=1\rightarrow L=3$, anticipating already at very weak coupling the strong-coupling result that this excitation energy should fall fastest, and collapse as $5/3g^2$. Unlike the $L=3$ state, the $L=2$ and $L=1$ excited states do not show any tendency to collapse onto the ground state in the large-g limit. Therefore they can be seen as modes involving essentially radial massive vibrations.

The next group of excitations is for $N_v=2$, and comprises $3\times 15=45$ states. This multiplet splits into seven levels corresponding to $L=5$, 3, 1, 4, 2, 1, and 3. The lowest ($L=5$) level crosses two levels of the lower ($N_v=1$) multiplet in its downwards motion to become the second excited state above the $L=3$ level, eventually constituting the low-energy odd-L rotational multiplet of the strong-coupling picture. The same route is followed by the lowest level of $N_v=3$, which is an $L=7$ state. In fact, all the lowest split levels from each N_v multiplet appear to have $L=2N_v+1$ and follow the same route. For $N_v=2$ we can similarly follow the movement with g of the $L=4$ level which decreases slowly toward the $L=2$ state from the lower $N_v=1$ to add to the group of massive radial vibrations.

B. $n=2,4$ electrons

Figure 5 has several features which contrast sharply with the one-electron case. The $N_v=0$ multiplet has 15 two-electron states. The spin-singlet subspace consists of a sixfold-degenerate multiplet that splits into an orbital S and a D multiplet. As the semiclassical Eq. (36) suggests, the ground state and lowest excitations in the strong-coupling limit have orbital degeneracies of *even* angular momenta. In fact, the lowest two among these states ($L=0,2$) both come from the $N_v=0$ multiplet, in contrast with the one-electron case. The next pseudorotational level ($L=4$) originates in the $6\times5=$ thirtyfold degenerate $N_v=1$, spin-singlet multiplet. Actually, at weak coupling it starts out being second in the ordering ($L=2,4,3,2,1,0$), but already at very small g it crosses the lower $L=2$ partner and approaches the pseudorotational asymptotic level. The convergence with increasing cutoff $N^{\max}$ is worse than in the $n=1$ case, which may be due to larger JT distortions associated with two electrons. The spin-triplet ($S=1$) states of $n=2$ have not been plotted, as they behave in exactly the same fashion as the $n=1$ states (see Fig. 4). This figure can be read in terms of $n=2$, $S=1$ states simply by replacing the spin-multiplicity label 2, used in the case $n=1$, with 3. By comparison of Fig. 5 and Fig. 4 we notice that the low-spin ^1P state of $N_v=1$ is exactly degenerate with the high-spin ^3D state in the same multiplet. This degeneracy seems accidental.

C. $n=3$ electrons

For three electrons, the results are shown in Fig. 6. The eightfold-degenerate $N_v=0$ multiplet splits into two states characterized by degeneracies 3 and 5 (^2P and ^2D). The ground state has the correct symmetry for an $L=1$, $k=0$ state, which is predicted to be the ground state in the semiclassical limit. We also expect the lowest excitations to be classified as $L=3$, $k=2$ (fourteenfold degenerate), and $L=3$, $k=0$ (sevenfold degenerate). In fact, three levels from the $N_v=1$ multiplet move down toward the ground state for increasing g. The one which moves lowest is ninefold degenerate (^2G). In the $g\to\infty$ limit, it must therefore merge with the fivefold levels from the $N_v=0$ multiplet to produce the expected $L=3$, $k=2$ pseudorotator excitation. The next excitation of the $L=3$, $k=0$ state can be identified as an asymptotic limit of the ^2F sevenfold-degenerate state seen in Fig. 6.

A remarkable feature of the $n=3$ case is the presence in the $N_v=1$ multiplet of a state (the ^2S) whose energy is independent of g. This state is degenerate with the $S=\frac{3}{2}$ state ^4D which has no JT distortion.

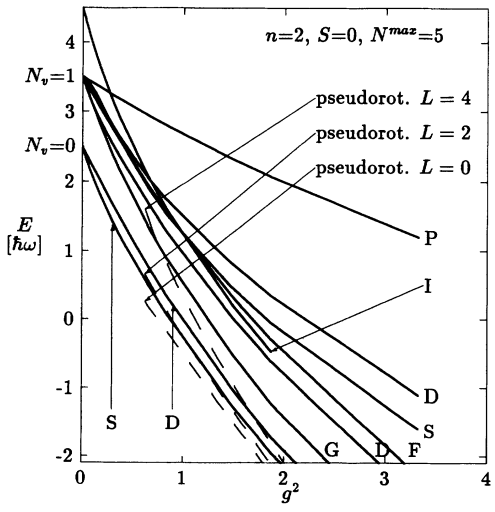

FIG. 5. Exact spectrum for two electrons ($S=0$). The semiclassical energies [Eq. (28)] are drawn by dashed lines for the lowest three pseudorotational multiplets ($n_\gamma=0,L=0,2,4$). The two-electron $S=1$ spectrum is the same as for $n=1$, $S=\frac{1}{2}$.

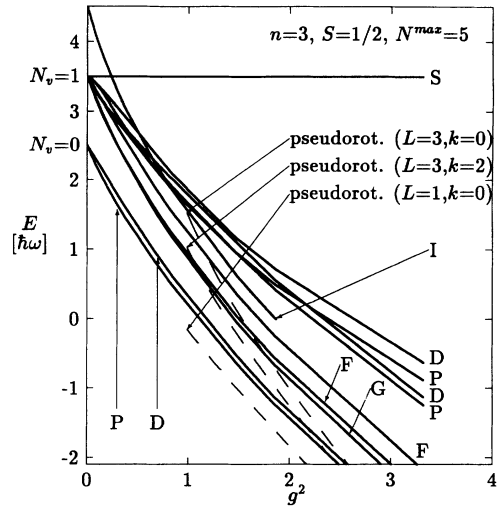

FIG. 6. Exact spectrum for three electrons ($S=\frac{1}{2}$). The semiclassical energies, Eq. (44), are drawn by dashed lines for the lowest three pseudorotational multiplets, $n_\gamma=0$ $(L,k)=(1,0),(3,2),(3,0)$.

VI. PAIR BINDING ENERGIES

The *pair energy* for an average filling of n electrons is defined as

$$U_n=E_{n+1}+E_{n-1}-2E_n\ , \tag{50}$$

where E_n are the fully relaxed ground-state energies of n electrons. Formally, U is the real part of the two-electron vertex function at zero frequency. If this energy is negative for odd values of n, it means that electrons will have lower total energy if they separate into $(n-1)$ and $(n+1)$ occupations of different molecules, rather than occupying n electrons on all molecules. For odd values of n, this is an effective pairing interaction often called "pair binding" in the literature.[5] In Sec. IV we found that, for all odd n, the pair energies are negative, and given by the large-g asymptotic expression

$$U_{n=1,3,5}\sim -g^2+1-\frac{2}{3g^2}\ . \tag{51}$$

The first term is the *classical energy*. The second term is due to reduction of the zero-point energy along the JT manifold, since only radial modes remain hard. This term is independent of g and positive. The last term is due to the quantum pseudorotator Hamiltonian, and the Berry phases which impose a finite ground-state energy associated with odd L for odd numbers of electrons. This term, although nominally small at large g, becomes important at weaker coupling. If (51) is extrapolated to the weak-coupling regime, the last term will dominate the pair binding energy. The exact diagonalization shown in Fig. 7 indeed shows a significant enhancement of the pair binding energy over the classical value in the weak-coupling regime.

In the weak-coupling limit, we can obtain analytical expressions for $U_n(g)$ for $g \ll 1$ by second-order perturbation theory. The unperturbed Hamiltonian is the noninteracting part H^0 with eigenstates (48). The perturbing Hamiltonian is $H^{e\text{-}v}$ of Eq. (7), which connects Fock states differing by one vibron occupation. All diagonal matrix elements vanish, and the leading-order corrections to any degenerate multiplet are of order g^2. These are given by diagonalization of the matrix,[25]

$$\Delta^{(2)}_{n_{ms},n'_{ms}} = \left\langle 0,n_{ms} \left| H^{e\text{-}v} \frac{1}{E_a^{(0)} - H^0} H^{e\text{-}v} \right| 0,n'_{ms} \right\rangle , \tag{52}$$

in the degenerate zero-vibron subspace. The sum implied by the inverse operator $(E_a^{(0)} - H^0)^{-1}$ extends just to the $N_v = 1$ states. The eigenvalues of $\Delta^{(2)}$ yield the ground-state energies and splittings for different electron fillings. These results, for all H_g and also A_g modes, and extended to the $N_v = 1$ multiplet, will be discussed more extensively in the following paper.[15]

Here we refer only to ground-state energetics. In particular, using the perturbative expressions, we obtain, for a single H_g mode, the small-g pair binding energy

$$\frac{U_{n=1,3,5,}}{\hbar\omega} = -\tfrac{5}{2}g^2 + O(g^4) . \tag{53}$$

The dependence strictly on powers of g^2 alone, with absence of all odd powers, is a consequence of the already mentioned $\Delta N_v = \pm 1$ selection rule of Eq. (7). The origin of the $\frac{5}{2}$ factor that characterizes the perturbative result (53) with respect to the classical pair binding energy (Table I) was also pointed out by Yabana and Bertsch[26] and will be further discussed in the following paper.[15]

The molecular pair binding energy can be considered as an effective negative-U Hubbard interaction for the lattice problem, provided that the Fermi energy ϵ_F is not much larger than the JT frequency scale ω. A mean-field estimate of the transition temperature for the negative-U Hubbard model in the weak-coupling regime is[27,5]

$$T_c \approx \epsilon_F \exp[(-N(\epsilon_F)|U|)^{-1}] , \tag{54}$$

where $N(\epsilon_F)$ is the density of conduction electron states. In Refs. 3 and 28, the results of the Migdal-Eliashberg approximation for the superconducting transition temperature were given. Without the Coulomb pseudopotentials this approach yields

$$T_c \approx \omega \exp[(-N(\epsilon_F)|V|)^{-1}] , \quad V = -\tfrac{5}{6}g^2 . \tag{55}$$

By comparing (53) to (55) we find a striking discrepancy between the values of the effective pairing interaction:

$$U = 3V . \tag{56}$$

That is to say, in the weak-coupling regime, the correct molecular calculation yields a pairing interaction which is *three times larger* than the results of Migdal-Eliashberg theory.

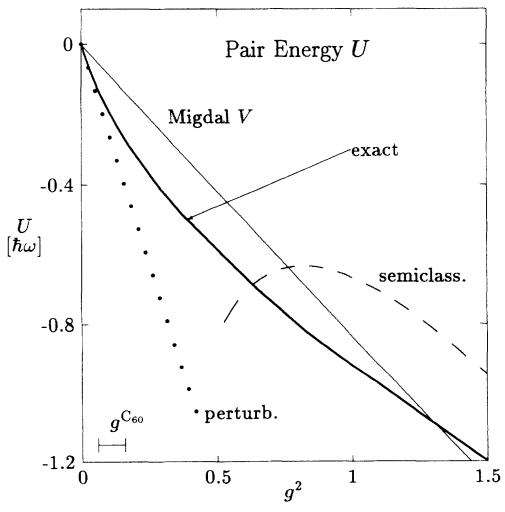

FIG. 7. Pair binding energy U (thick solid line), compared to weak-coupling perturbation theory for $g \ll 1$ (dotted line) and semiclassical theory for $g \gg 1$ (dashed lines). U_n is found to be the same for $n = 1,3,5$ electrons. The Migdal-Eliashberg approximation V (thin solid line) is also drawn for comparison. $g^{C_{60}}$ is the range of physical coupling strength for C_{60}.

VII. DISCUSSION

In this paper, we have solved the problem of a single H_g vibron coupled to t_{1u} electrons in a C_{60}^{n-} molecule. The model is too simplified for quantitative predictions for C_{60}, but it contains interesting physics which will be important for further studies of this system.

Semiclassically, a dynamical Jahn-Teller effect occurs. For $n = 1,2,4,5$, the molecule distorts unimodally, giving rise to a pseudo-angular-momentum spectrum, plus three harmonic oscillators. For $n = 3$, there is a bimodal distortion, which generates a spectrum of a symmetric top rotator, plus two harmonic oscillators. The pseudorotations are subject to nontrivial Berry-phase effects, which determine the pseudo-angular-momenta L, and thus the degeneracies and level ordering of the low-lying states. Strong Berry-phase effects seem to survive even at moderate and weak coupling, as shown by the exact diagonalization results.

We find at weak coupling that the pair binding energy is a factor of $\frac{5}{2}$ larger than the classical JT effect, and a factor of 3 larger than the pairing interaction of the Migdal-Eliashberg theory of superconductivity. This enhancement can be interpreted semiclassically as due to

the large zero-point energy reduction of the pseudorotations. From the weak-coupling point of view, this effect is due to degeneracies in both electronic and vibronic systems.

Migdal's approximation neglects vertex corrections in the resummation of two-particle ladder diagrams. This is justified only in the retarded limit $\omega \ll \epsilon_F$. Here we have considered the opposite limit, where the molecular ground-state energies are solved first, assuming that the JT relaxation time is of the same order, or faster than the intermolecular hopping time. In this regime, we have found therefore that Migdal's approximation substantially *underestimates* the pairing interaction, and T_c, for these ideal molecular solids.[29] This large effect suggests that some of the enhancement is likely to carry over to the real case of A_3C_{60} metals, where electron-hopping t and vibron frequencies are of similar strength.

In the following paper, part II, we shall consider a more realistic model which includes all important vibron modes of C_{60}. We shall present quantitative predictions for the electron-vibron effects on the spectroscopy of C_{60} ions.

ACKNOWLEDGMENTS

A.A. is indebted to Yossi Avron and Mary O'Brien for valuable discussions, and acknowledges the Sloan Foundation for support. E.T. and N.M. wish to acknowledge discussions with S. Doniach. This paper was supported by grants from the U.S.-Israel Binational Science Foundation, the Fund for Promotion of Research at the Technion, and the U.S. Department of Energy No. DE-FG02-91ER45441, the Italian Istituto Nazionale di Fisica della Materia INFM, the European U.S. Army Research Office, the EEC through Contract No. ERBCHRXCT 920062, and NATO through CRG 920828.

*Electronic address: assa@phassa.technion.ac.il
†Electronic address: manini@tsmi19.sissa.it
‡Electronic address: tosatti@tsmi19.sissa.it

[1]A. F. Hebard, Phys. Today **45**(11), 26 (1992), and references therein.
[2]C. M. Varma, J. Zaanen, and K. Raghavachari, Science **254**, 989 (1991).
[3]M. Schlüter, M. Lannoo, M. Needels, G. A. Baraff, and D. Tománek, Phys. Rev. Lett. **68**, 526 (1991); J. Phys. Chem. Solids **53**, 1473 (1992).
[4]R. A. Jishi and M. S. Dresselhaus, Phys. Rev. B **45**, 2597 (1992); M. G. Mitch, S. J. Chase, and J. S. Lannin, *ibid.* **46**, 3696 (1992).
[5]G. Baskaran and E. Tosatti, Curr. Sci. (Bangalore) **61**, 33 (1991); S. Chakravarty, M. Gelfand, and S. Kivelson, Science **254**, 970 (1991); G. N. Murthy and A. Auerbach, Phys. Rev. B **46**, 331 (1992).
[6]K. H. Johnson, M. E. McHenry, and D. P. Clougherty, Physica C **183**, 319 (1991).
[7]C. A. Mead, Rev. Mod. Phys. **64**, 51 (1992).
[8]*Geometric Phases in Physics,* edited by A. Shapere and F. Wilczek (World Scientific, Singapore, 1989).
[9]H. C. Longuet-Higgins, Adv. Spectrosc. **2**, 429 (1961), and references therein; G. Herzberg and H. C. Longuet-Higgins, Discuss. Faraday Soc. **35**, 77 (1963); H. C. Longuet-Higgins, Proc. R. Soc. London, Ser. A **344**, 147 (1975); C. A. Mead and D. G. Truhlar, J. Chem. Phys. **70**, 2284 (1979).
[10]G. Delacrétez, E. R. Grant, R. L. Whetten, L. Woste, and J. W. Zwanziger, Phys. Rev. Lett. **56**, 2598 (1986).
[11]B. Goss Levi, Phys. Today **46** (3), 17 (1993).
[12]E. Tosatti (unpublished).
[13]J. Gonzalez, F. Guinea, and M. A. H. Vozmediano, Phys. Rev. Lett. **69**, 172 (1992).
[14]J. Ihm (unpublished).
[15]N. Manini, E. Tosatti, and A. Auerbach, following paper, Phys. Rev. B **49**, 13008 (1994).
[16]A. R. Edmonds, *Angular Momentum in Quantum Mechanics* (Princeton University, Princeton, 1974).
[17]M. C. O'Brien, Phys. Rev. **187**, 407 (1969).
[18]M. C. M. O'Brien, J. Phys. C **4**, 2524 (1971).
[19]One should not confuse the pseudorotations of Eq. (22), which describe propagating vibrational waves, with real rotations of the molecule. In the solid state those are assumed to be frozen out by crystal fields at the temperatures of interest. Moreover, for a real rigid body, each moment of inertia cannot exceed the sum of the other two (Ref. 30).
[20]L. D. Landau and E. M. Lifshitz, *Quantum Mechanics* (Pergamon, Oxford, 1976), Chap. 13.
[21]F. S. Ham, Phys. Rev. Lett. **58**, 725 (1987).
[22]V. P. Antropov, A. Gunnarsson, and A. I. Liechtenstein, Phys. Rev. B **48**, 7651 (1993).
[23]O. Gunnarsson, D. Rainer, and G. Zwicknagl, in *Clusters and Fullerenes,* edited by V. Kumar, T. P. Martin, and E. Tosath (World Scientific, Singapore, 1993), p. 409.
[24]Z. Gasyna, L. Andrews, and P. N. Schatz, J. Phys. Chem. **96**, 1525 (1991).
[25]J. J. Sakurai, *Modern Quantum Mechanics* (Benjamin, Menlo Park, CA, 1985).
[26]K. Yabana and G. Bertsch, Phys. Rev. B **46**, 14 263 (1992).
[27]V. J. Emery, Phys. Rev. B **14**, 2989 (1976); A. Aharony and A. Auerbach, Phys. Rev. Lett. **70**, 1874 (1993).
[28]M. Lannoo, G. A. Baraff, and M. Schlüter, Phys. Rev. B **44**, 12 106 (1991).
[29]Our reason for the enhancement is different from those of other recent discussions of breakdown of the Migdal-Eliashberg approximation [see, e.g., L. Peitronero, Europhys. Lett. **17**, 365 (1992)].
[30]L. D. Landau and E. M. Lifshitz, *Mechanics* (Pergamon, Oxford, 1960), Chap. 32.